Fracture behavior of plain and fiber-reinforced high strength concrete containing high strength steel fiber

P.N. Ojha, Pranay Singh, Brijesh Singh, Abhishek Singh, Piyush Mittal

To cite this article

Disclaimer

Research Article

Fracture behavior of plain and fiber-reinforced high strength concrete containing high strength steel fiber

P.N. Ojha[a], Pranay Singh[b], Brijesh Singh[*c], Abhishek Singh[d], Piyush Mittal[e]

National Council for Cement and Building Materials, India

Article Info	Abstract
	With the increase in strength, concrete explodes spontaneously at failure creating a serious safety hazard. Researchers are actively looking for methods to arrest the cracks in concrete and design a higher strength concrete that fails in a more ductile fashion. Fiber-reinforced concrete has emerged as one of the solutions to this problem. This paper presents findings from the experimental investigation conducted to compare the fracture behavior of plain and fiber-reinforced high strength concrete of varying compressive strength. Six different concrete mixes were prepared with w/b ratios of 0.47, 0.36, and 0.20 resulting in average compressive strength of 36, 52, and 92 MPa. Each mix consists of two variations, first without fiber and second with 1% of steel fiber by volume. The mixes were tested for their strength and fracture Behavior using various standard codes and recommendations. From the Load-deflection and Load-CMOD (Crack Mouth Opening Displacement) curves obtained from the study, Fracture parameters like Fracture energy, Stress intensity factor, energy release rate, and Characteristic length is evaluated and compared for plain and Steel fiber reinforced concrete. It was found that adding steel fiber significantly improves the fracture properties of the concrete of different compressive strengths. By adding 1% of steel fiber in the high-strength concrete, the average fracture energy increased by 850%, 770%, and 450% respectively for the concrete with compressive strength of 36, 52, and 92 MPa. Other parameters also show a very significant improvement suggesting fiber reinforcement as a suitable choice to prevent brittle failure and increase the fracture performance of high strength concrete.

1. Introduction

Concrete shows many desirable properties like good compressive strength, high durability, ability to be cast in any shape, and comparatively lower cost than other construction materials. All these qualities have made concrete a universal construction material almost integral to every construction project. But one of the major limitations of concrete is its brittle nature and low crack resistance. This limits its ability to take the flexural load and makes it extremely dangerous under extreme events like earthquakes[1, 2]. Due to this weakness, concrete structures under flexural loads are susceptible to getting cracked and fail spontaneously without warning. The strain capacity of concrete further reduces for high strength concrete. High strength concrete shows better properties in terms of compressive strength, Abrasion, toughness, and impact than normal concrete[3–5]. But its ductility and crack resistance reduce drastically with strength increase, leading to sudden failure.

One of the quantitative estimations of brittleness and ductility of concrete is its fracture properties. RILEM [6, 7] proposes a three-point bending test on a notched beam to find the

fracture parameters for concrete. Fracture energy is one of the most important fracture parameters and it can be defined as a parameter to analyze and compare the toughness and cracking resistance of the concrete. As per RILEM, Fracture energy is the amount of energy necessary to create a unit area of crack [6]. Other fracture parameters are fracture toughness, Energy release rate, and characteristic length. Fracture toughness refers to the resistance of brittle materials to the spread of cracks. The energy release rate is the rate at which the energy is transformed with the fracture propagation in the material. Characteristic length is one of the measures of the brittleness of the concrete, a concrete can be considered more brittle if it shows a lower characteristic length [8].

Various work has been done in past to measure these fracture parameters and correlate them with the ductility and crack resistance of the concrete. Trevidi et al. [9] compared three different approaches i.e., Rilem method, Bi-linear approximation, and energy release rate to investigate the size-independent fracture energy of concrete and found almost similar results suggestion any one of these can be used to calculate the size-independent fracture energy of concrete. Khalilpour et al. [10] further compared the number of available methods of determination of fracture parameters and reviews the factors affecting these parameters. Yin et al. [11] presents Four-point bending tests for the fracture properties of concrete. Murthy et al. [12] studied the fracture energy and tension softening relation for nano-modified concrete. This study compared the different methods of fracture energy determination and concluded that the notch to depth ratio has a significant impact on the specific fracture energy determined using the RILEM work-of-fracture technique. Kaya et al. [13] studied the effects of temperature and deformation rate on fracture behavior of S-2 glass/epoxy laminated composites. The study presents a Finite Element Method based approach to find the fracture parameters and compares the experimental and FEM-based results.

The effect of adding different types of fibers in the concrete on its fracture behavior has been discussed by many researchers. Almusallam et al. [14] performed an analytical and experimental investigation on fracture behavior of concrete containing steel, Kevlar, and polypropylene and found better fracture properties. Mousavi et al. [15] studied fracture properties of concrete under varying steel fiber content as well as water to cementitious content ratio and suggests that with the decrease in w/b ratio fracture energy decreases for plain concrete but increases for fiber reinforced concrete. Arslan [16] studied the fracture behavior of basalt fiber reinforced concrete (BFRC) and glass fiber reinforced concrete (GFRC). BF and GF addition considerably increase the fracture energy of test specimens compared to Reference specimens. Noaman et al. [17] studied the Fracture characteristics of plain and steel fiber reinforced rubberized concrete. Only up to a certain degree of replacement does the fracture energy of plain and steel fiber concrete rise. Because of the loss of strength in the cement matrix, the fracture energy decreases slightly after this replacement ratio. The fracture energy of plain concrete is significantly increased when rubber aggregate is combined with hooked-end steel fiber. Wtaife et al. [18] studied the Fracture Mechanism of fiber Reinforced Concrete Pavement based on a RILEM Design Approach. Despite having relatively low ultimate moment capacities, the ultimate moment capacities increase as the volume fraction of fiber increases.

Studies on the effect of silica fume and fly ash addiction along with cement as a binder material in concrete and aggregate size distribution on its fracture behavior are reported by various researchers. Gil et al. [19] studied the effect of Silica Fume and Siliceous Fly Ash Addition on the Fracture Toughness of Plain Concrete. His finding suggests an optimum dose of Silica fume and Flyash for maximum strength and fracture toughness. Siregar et al. [20] studied the effects of aggregate size distribution on the fracture behavior of high-strength concrete. The ductility level of high-strength concrete is influenced by the

aggregate size distribution and w/b ratio also the maximum value of fracture energy is related to the maximum strength of the aggregate.

Fracture properties variations on concrete exposed to higher temperatures have been studied in past. Tang et al. [21] examined Fracture behavior of recycled concrete with waste crumb rubber subjected to elevated temperatures. At ambient temperature Rubber modified Recycled aggregate concrete (RRAC) shows an increasing trend in fracture energy with increasing content of recycled aggregate. After exposure to high temperature, the fracture energy of RRAC was lower than Rubber modified Natural aggregate concrete (RNAC). With the increase in temperature, a decrease in fracture energy was reported in the study. Yu et al. [22] studied the Fracture properties of high-strength/high-performance concrete (HSC/HPC) exposed to high temperatures. Concrete's characteristic lengths dropped linearly with the temperature rise, indicating a reduction in brittleness. At all temperatures, the characteristic length of lower strength concrete sample was greater than that of a higher strength sample, indicating that the brittleness of concrete increased with compressive strength.

Tran et al.[23] Fracture energy of ultra-high-performance fiber-reinforced concrete (UHPFRC) at high strain rates. The UHPFRCs' fracture strength and specific work-of-fracture values were extremely sensitive to the applied strain rates, but their softening fracture energies were not much affected. The fracture process of recycled concrete was thoroughly investigated by Guo et al. [24] and compared to that of conventional concrete of the same structural class. In recycled aggregate concrete, higher strain gradients are seen in the localized damage zone. Strong discontinuities or existing fractures in recycled aggregate aid in the identification of the primary crack. Because fracture occurs at the aggregate-mortar interface, the recycled aggregate concrete's larger strain gradient and poor stiffness suggest a weak interface between the new mortar and recycled aggregate, which is attributed to excessive porosity and existing fractures.

In the present study, six different mixes were prepared with three w/b (water to binder) ratios. The w/b ratios adopted are 0.47, 0.36 and 0.20. These three mixes represent concrete with compressive strength above 30 MPa, 50Mpa, and 90 MPa. For each of these w/b ratios, two sets of concrete samples were prepared – one without steel fiber and one with 1% steel fiber by volume. Using the three-point bend test suggested by RILEM[6] and Tada et al. [25], fracture energy is calculated. Other fracture parameters like characteristic length, critical energy release rate, and stress intensity factors are evaluated using literature [7, 25–28]. The results are compared for plain and fiber reinforced concrete. Apart from these, 28-day cube and cylindrical compressive strength and split tensile strength are also evaluated for each sample using the Indian Standard code [29, 30].

2. Materials

In this study OPC cement, Coarse and Fine aggregates, Fly ash, Silica Fumes, Superplasticizer, water, and steel fiber are used for making concrete mixes. This section provides details of the materials used in the study.

2.1. Cementitious Materials

Ordinary Portland Cement of OPC 53 grade as per IS 269-2015 [32] is used along with fly ash and silica fume. 28-day compressive strength of cement was 36.0 MPa and specific gravity was 3.16. Fly ash and silica fume have the fineness of 403 and 22000 and specific gravity of 2.2 and 2.24 respectively. Detailed physical and chemical properties of cement, fly ash, and silica fume is given in Table 1.

Table 1. Physical, chemical and strength characteristics of cementitious materials

Characteristics	OPC -53 Grade	Silica Fume	Fly Ash
Physical Tests			
Fineness Blaine's (m²/kg)	320.00	22000	403
Soundness Autoclave (%)	00.05	-	-
Soundness Le Chatelier (mm)	1.00	-	-
Setting Time Initial (min.) & (max.)	170.00 & 220.00	-	-
Specific gravity	3.16	2.24	2.2
Chemical Tests			
Loss of Ignition (LOI) (%)	1.50	1.16	0.4
Silica (SiO_2) (%)	20.38	95.02	60.95
Iron Oxide (Fe_2O_3) (%)	3.96	0.80	5.70
Aluminium Oxide (Al_2O_3)	4.95	-	26.67
Calcium Oxide (CaO) (%)	60.73	-	2.08
Magnesium Oxide (MgO) (%)	4.78	-	0.69
Sulphate (SO_3) (%)	2.07	-	0.29
Chloride (Cl) (%)	0.04	-	0.009
IR (%)	1.20	-	-
Moisture (%)	-	0.43	-

2.2. Aggregates

Crushed aggregate with a maximum nominal size of 20mm is utilized as coarse aggregate and crushed fine aggregate conforming to Zone II as per IS: 383-2016 [33] was employed as fine aggregate in the study. Fine aggregate has been shown in figure 1(a) and figure 1(b) shows the coarse aggregate. The physical properties of both coarse and fine aggregate are presented in Table-2.

Fig. 1 (a) Crushed fine aggregate (b) Granite coarse aggregate

Table 2. Properties of aggregates

Property		Granite		Fine Aggregate
		20 mm	10 mm	
Specific gravity		2.83	2.83	2.65
Water absorption (%)		0.3	0.3	0.59
Sieve Analysis Cumulative Percentage Passing (%)	20mm	98	100	100
	10 mm	1	68	100
	4.75 mm	0	2	99
	2.36 mm	0	0	89
	1.18 mm	0	0	64
	600 μ	0	0	43
	300 μ	0	0	26
	150 μ	0	0	14
	Pan	0	0	0
Abrasion, Crushing & Impact Value		19,19,13	-	-
Flakiness % & Elongation %		29, 25	-	-

2.3. Steel Fiber

The trough and hooked end-shaped steel fibers are used. Some of the previous studies suggest these fibers be more efficient with improved pull-out resistance and toughness compared to straight end fibers. The fibers are 0.55 mm in diameter and 35 mm in length. It has an aspect ratio of 63 which is as per ASTM A-820 [34]. The tensile strength of the fibers as per the manufacturer is 1486.99 N/mm^2. Figure 2 shows the steel fiber added to the concrete mix. The figure on the left shows the fibers as available from the industry and the figure on the right shows a single steel fiber.
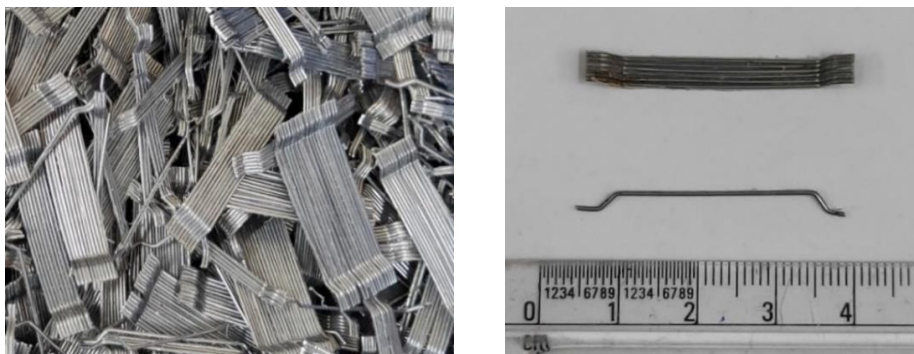

Fig. 2 Steel Fiber added to the concrete

2.4. Superplasticizer

A polycarboxylic group-based superplasticizer is used in the study for all the w/b ratios as per Indian Standard IS:9103[35].

3. Mix Design and Specimen Details

3.1. Mix Design

Six different sets of mixes were prepared with a w/b ratio of 0.47, 0.36, and 0.20. These different types of concrete mixes were prepared in two variations-(i) plain concrete and (ii) concrete with 1% steel fiber. The fresh concrete's slump was regulated between 75 and 100 mm. Based on the slump cone test as per Indian Standard, IS 1199: Part 2 [36], a pre-study was conducted to identify the best superplasticizer dose for obtaining the requisite workability. The amount of steel fiber added to the concrete was adopted based on past studies suggesting it as an economical and optimum dose for maximum improvement in overall mechanical parameters [35, 36].

Table 3 lists the concrete mix data for the sample. Water content has been decreased and cementitious content has been increased to get a higher strength concrete. Also, in the case of a mix with a w/b ratio of 0.20, silica fume has been added to obtain a much higher strength of the concrete. Silica fume was added to improve the mechanical properties, particularly the compressive strength of high-strength concrete [39].

Table 3. Mix design details

Fibers % by volume of concrete	w/b	Total Cementitious Content [Cement C + Flyash (FA) + Silica Fume (SF)] (Kg/m³)	Ratio of silica fume to flyash (SF /FA)	Water Content (Kg/m³)	Admixture % by weight of Cement	Fine Aggregate as % of Total Aggregate by weight
Without Fibers	0.47	362 (290+72+0)	-	170	1.00	35
	0.36	417 (334+83+0)	-	150	0.45	39
	0.20	750 (548+112+90)	0.80	150	1.75	35
1% steel fiber	0.47	362 (290+72+0)	-	170	1.00	35
	0.36	417 (334+83+0)	-	150	0.45	39
	0.20	750 (548+112+90)	0.80	150	1.75	35

As an adjustment for aggregate water absorption, a change was made to the amount of added water. The concrete mixes for the investigations were made in a pan-type concrete mixer. The molds were adequately coated with mineral oil before usage, and casting was done in three layers, each of which was compressed on a vibration table to reduce air bubbles and voids. The specimens were removed from their separate molds after 24 hours. Temperature and relative humidity were measured in the laboratory at 27°+2° C and relative humidity of 65 percent or greater at various ages. The specimens were removed from the tank and allowed to dry on the surface before being tested in a saturated surface dried state.

3.2. Specimen Details

Different specimens were made for different tests as per specifications in the standard codes, international recommendations, and literature.

Concrete cubes of size 150 mm x 150 mm x 150 mm are cast to find 28-day compressive strength as per IS 516[30].

Concrete cylinders of size 150 mm diameter and 300 mm height are cast to find the 28-days compressive strength of the concrete as per IS 516[30].

Concrete beams of size 100mm x 100mm x 500mm are cast for a 3-point bending test at 28-days to evaluate the fracture parameters using various proposed procedures as

discussed in the introduction section. 24 hours before testing a notch of 35mm is made in the beam. Table 4 shows specimen details and Figure 3 shows the freshly prepared concrete specimens in molds.

Table 4. Specimens details and experiments in the study

S.No.	Specimen	Dimension(mm)	Tests
1	Concrete Cubes	150 x150 x 150	28-Day compressive strength
2	Concrete Cylinders	150D x 300H	28-Day compressive strength Split Tensile strength
3	Concrete Beams	100 x 100 x 500	3 – Point bend test to evaluate fracture Parameter

Fig. 3 Concrete cubes, cylinders, and beams in molds

Fig. 4 Notched beam sample

4. Experimental Procedure

The following section details the adopted procedures for conducting the experiments. In the present study compressive strength test, split tensile strength test and 3-Point bend test on notched beams are performed. Findings and derivation of other parameters are given in the next section, i.e., the results and discussion section.

4.1. Compressive strength test and split tensile strength test

The compressive strength of cylindrical and cubical specimens was evaluated at 28-days as per IS: 516 [30]. And the split tensile strength of the cylindrical concrete specimen was evaluated as per the testing procedure of IS: 5816-1999 [31] on the cylindrical specimen at 28 days. These tests were performed on a set of three specimens and the average value has been presented in the study.

4.2. Three-point bending test to evaluate fracture parameters

For calculating the fracture parameters, a 3-point bending test based on the method proposed by RILEM [6, 7] was used. Various fracture parameters were evaluated from the tests and are discussed in the subsequent sections. Figure 5 shows a schematic diagram for the three-point bend test and figure 6 shows the laboratory arrangement for the conducted test. As presented in figure 5, a beam of dimension 100mm x 100mm x 500mm with a notch of 35mm at the mid-span was used. 400 mm of the clear span was considered and the load

was applied using a displacement control machine of capacity 300 Kn. Deflection at the mid-span of the beam was measured using LVDT and Crack Mouth Opening Displacement (CMOD) was measured using clip gauge placed at the bottom of the beam and fixed in position by two steel knife edges as shown in figure 6(b). In the present study, a total of eighteen beams has been tested which includes 3 beams for each of the mix presented in Table 3.
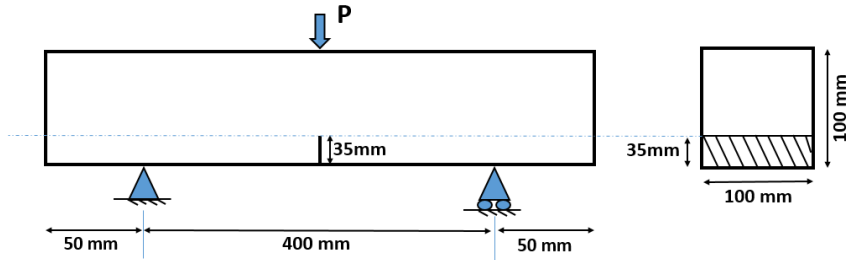

Fig. 5 Sample specification for 3-point bending test
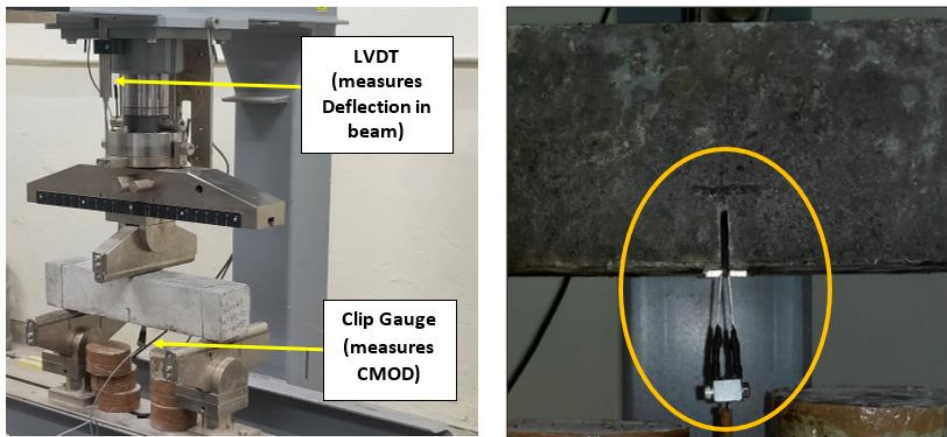
Fig. 6 (a) Test setup three-point bending test, and (b) Clip gauge measuring CMOD
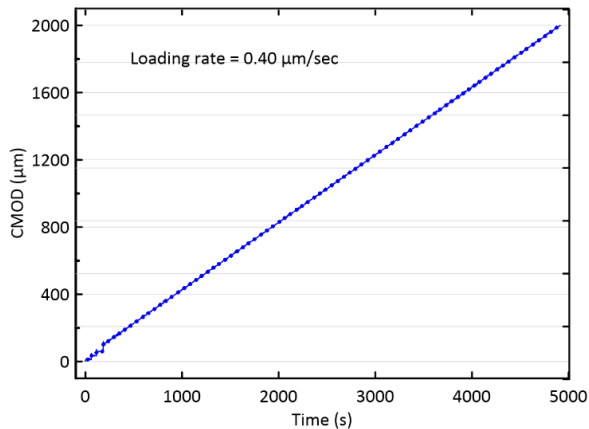
Fig. 7 CMOD vs time plot for the test

Figure 7 shows the CMOD vs time plot for the test. As described earlier the displacement-controlled test was adopted for this study and load was applied in such a manner that gives a constant increase in CMOD (0.40µm/s) with time as shown above. The test was performed till the beam failed or a maximum CMOD of 2000 µm is reached.

5. Results and Discussions

5.1. Compressive strength test and split tensile strength test

The cube compressive strength of mix with w/b ratio of 0.47, 0.36, and 0.20 are 37 MPa, 53 MPa, and 92 MPa respectively. Adding steel fiber does not considerably increase the compressive strength and only a marginal increase of not more than 10% is observed for any of the mixes. A similar marginal increase is observed in the split tensile strength of the mixes with and without steel fiber. By addition of steel fiber, split tensile strength of the mix with w/b ratio 0.47, 0.36, and 0.20 increased by 2%, 2%, and 4% respectively. Table 5 shows the results of the cube and cylindrical compressive strength and split tensile strength.

Table 5. Cube and cylindrical compressive strength and split tensile strength

W/B ratio	Type	28-day strength (MPa)		
		Cube Strength	Cylinder strength	Split Tensile Strength
0.47	Plain	36.90	27.62	3.37
0.47	Steel fiber	37.40	28.25	3.95
0.36	Plain	51.60	39.30	4.04
0.36	Steel fiber	53.20	44.87	4.73
0.2	Plain	92.20	78.29	5.35
0.2	Steel fiber	91.70	68.97	7.19

5.2 Load-Deflection and Load-CMOD Behavior

In the present section, the Load-Deflection and Load-CMOD behavior of three beams each for a w/b ratio (0.47,0.36 and 0.20) and fiber content (0% and 1%) is presented in figure 8, 9, and 10 respectively. As can be seen from these diagrams that for the w/b ratio of 0.47, the curve is uneven for fiber-reinforced beam, and it smoothies as the strength increases. The possible cause for this behavior can be attributed to the slipping of fiber from the concrete and uneven load distribution and sudden load transfer among concrete and fibers with the increase in CMOD at a lower strength. At higher strength, fibers and concrete matrix act as a single unit resulting in a smoother curve.

Another important observation is the variability of the results for fiber-reinforced beams. As can be seen in the plots that all the three beams of normal strength concrete show almost a similar characteristic in their behavior suggesting homogeneity in all three beams. But this cannot be assured for the fiber reinforced concrete as the orientation and distribution of fibers cannot be perfectly homogenized for all three beams. With the addition of steel fiber, the strain capacity of the beam increases, and with the increase in compressive strength, Peak-load increases. Both of these factors increase the area under the load-deflection curve increasing the fracture energy as discussed in the next section.
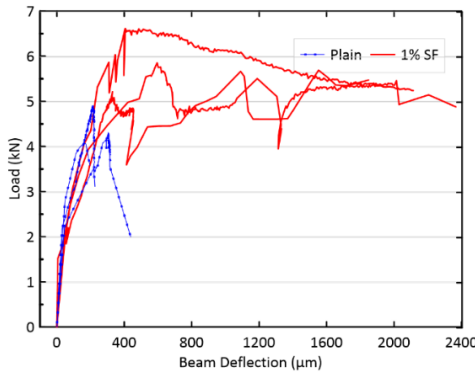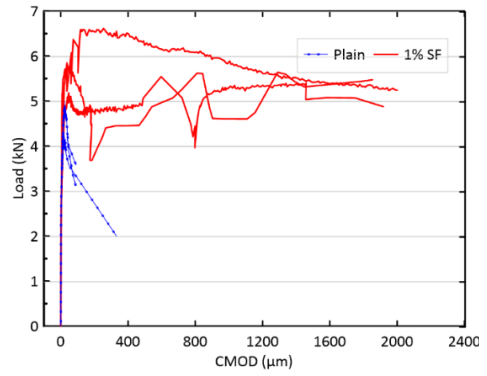
(a) Load - deflection curve   (b) Load CMOD curve

Fig. 8 W/B ratio 0.47
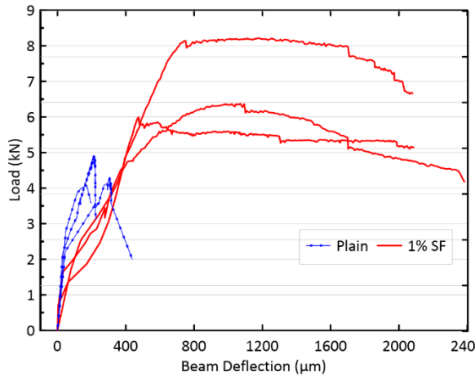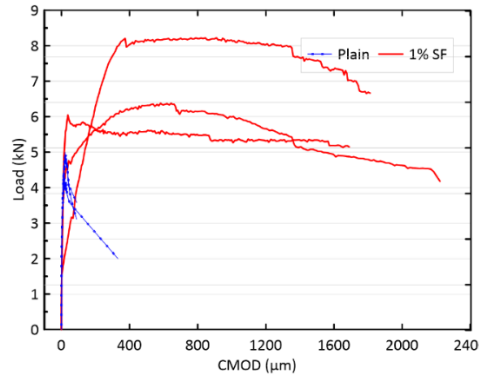
(a) Load - deflection curve   (b) Load CMOD curve

Fig. 9 W/B ratio 0.36
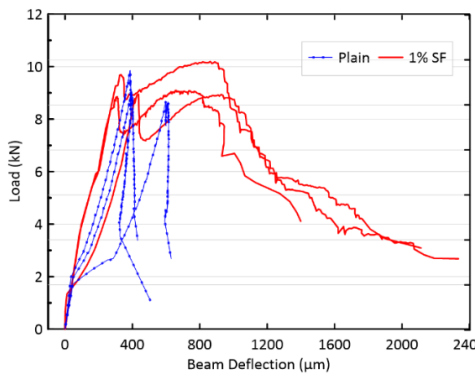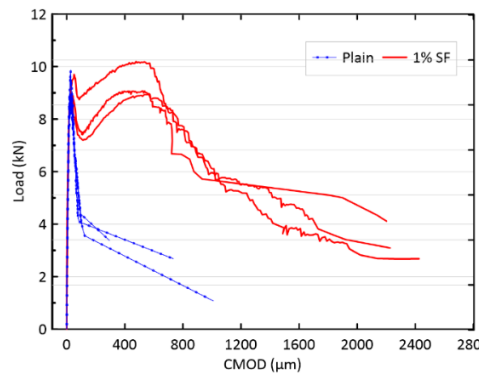
(a) Load - deflection curve   (b) Load CMOD curve

Fig.10 W/B ratio 0.20

5.3 Fracture Energy

Fracture energy, represented as G_f is defined as the energy required to produce a unit crack in the specimen. It is one of the basic properties of the material which can be used to analyze and determine the toughness, brittleness, and cracking resistance of the concrete. From RILEM 50-FMC [6] fracture energy can be calculated from the equation (1);

$$G_f(N/m) = (W_o + mg\delta_o)/A_{lig} \tag{1}$$

Here in equation (1) G_f refers to the fracture energy, W_o is the area under the load-deformation curve for the beam as shown in figure 7. m is the total weight of the beam between the support and weight of the part of loading arrangement which is not attached to the machine, but follows beam until failure. g is the acceleration due to gravity, i.e., 9.81 m/s^2. δ_o is the deformation of the beam at the final stage of failure and A_{lig} is the area of the ligament which is the area of the projection of fracture zone on the plane perpendicular to the beam axis, as represented by the shaded region in Figure 11.
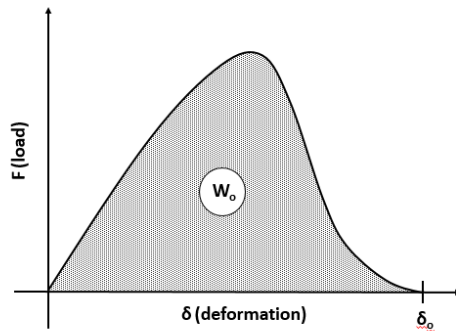

Fig. 11 Area under force and beam mid-point deflection (deformation) curve
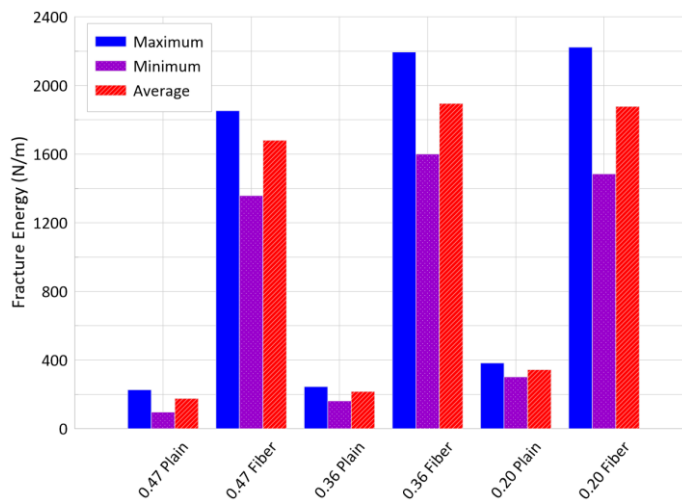
Fig. 12 Obtained fracture energy for w/b ratio of 0.47, 0.36 and 0.20

Figure 12 depicts a comparison between the obtained fracture energy for mix with different w/b ratios and fiber content. As can be observed from the figure addition of fibers significantly increases the fracture energy of the notched beam. An increasing trend in fracture energy can also be with an increase in concrete's compressive strength. An increase in fracture energy due to fiber addition is caused by a much larger strain value for the fiber-reinforced beam than the normal beam. And with the increase in compressive strength the maximum load taking capacity of the beam increases which results in higher fracture energy. The increase in fracture energy is about 9.5 times for the w/b ratio of 0.47, whereas it is only 8 times for 0.36 and 5 times for 0.20. With the increase in compressive strength relative benefit of adding fiber reduces because concrete at higher strength is itself capable of taking a higher bending load than a low strength concrete.

Previous literature [26] suggests an increase of about 8 times in fracture with the addition of steel fiber in normal concrete. The fracture energy reported for a concrete sample with compressive strength of 54 MPa was 271.4 N/m which increased to 2183.0 N/m, similar results were observed in our study also.

5.4 Initial Compliance and Modulus of Elasticity

The Modulus of Elasticity of the notched beams is calculated using equation (2) as presented by [38].

$$E\ (MPa) = 6S\ \frac{\alpha V_1(\alpha)}{C_i d b^2} \tag{2}$$

Where C_i is the initial compliance which is the inverse of the slope of the initial straight portion of the Load vs CMOD curve. Figure 13 shows the calculation of the slope of the initial straight portion of the Load-CMOD curve. $V_1(\alpha)$ is calculated using the equation (3) given by Tada et al. [25] as follow:

$$V_1(\alpha) = 0.76 - 2.28a + 3.87a^2 - 2.04a^3 + \frac{0.66}{(1-a)^2} \tag{3}$$

Table 6. Initial compliance and modulus of elasticity

W/ B ratio and fiber	Cube compressive strength (MPa)	Initial compliance C_i (10^{-9} m/N)	Modulus of elasticity(GPa) [cmod test]	Modulus of elasticity (GPa) [Arora et al.][3]
0.47 Plain	36.90	5.26	31.08	29.52
0.47 Fiber	37.40	4.54	35.17	29.64
0.36 Plain	51.60	5.0	32.27	32.64
0.36 Fiber	53.20	4.0	40.55	32.94
0.20 Plain	92.20	2.63	60.61	38.85
0.20 Fiber	91.70	2.22	72.63	38.79

Table 6 shows the calculated values of initial compliance and Young's modulus as obtained in the test and derived from the empirical equation given by [3]. As observed from table 6 calculation of modulus of elasticity from initial compliance give a higher value than the studies conducted in the past[3, 8], therefore Load-CMOD compliance-based approach does not seem to be a highly accurate method of determining the modulus of elasticity, therefore for the subsequent calculations in the study modulus of elasticity values obtained by Arora et al. [3]. Deterministic evaluation of the absolute value of the modulus of elasticity from the three-point bend test proposed by RILEM is extremely difficult due to the required level of sensitivity of the measurement. The proposed Load-CMOD curve and initial compliance are extremely sensitive and it requires accurate measurement of the

order of 10^{-9} m in a mechanical bend test. Even a slight variation in the initial slope of the Load-CMOD curves leaves a magnified effect in the values of modulus of elasticity. Also, calculated values of modulus of elasticity were higher than established previous results. These values tend to become enormously high for higher strength concrete (for average compressive strength of 92 MPa). It can be suggested to limit this method only for comparative analysis and for absolute determination of modules of elasticity various other well-established methods should be used.
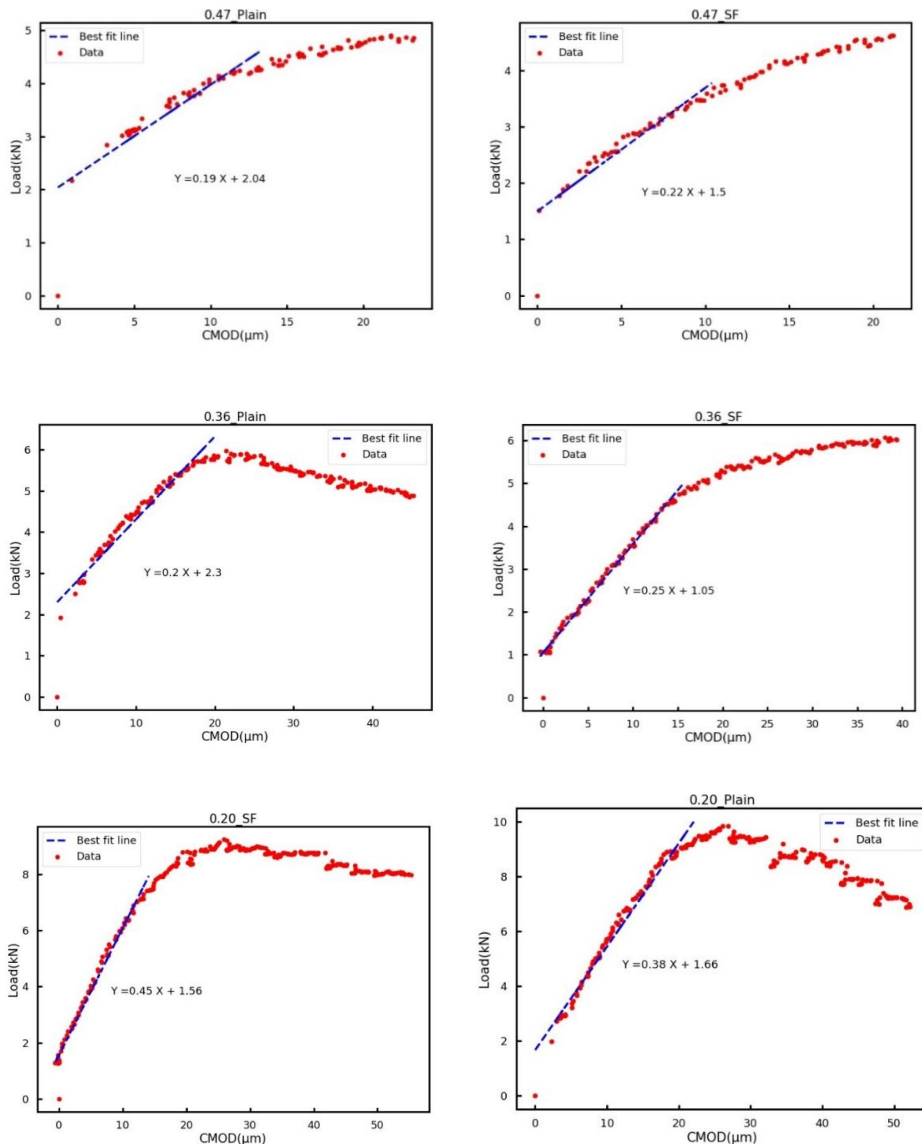

Fig. 13 Calculation of initial compliance from Load-CMOD curves

5.5 Stress Intensity Factor

The stress intensity factor (K_{IC}) is a measure of stresses in the neighborhood of a crack. It is a measure to predict the stress intensity caused by the residual stresses near the tip of a notch or crack. It can also be used to compare the brittleness of two different materials. Higher (K_{IC}) means that the material can allow higher stresses around the crack, suggesting a less brittle behavior.

The stress intensity factor is calculated using the equation (4), given by RILEM TC 89-FMT [7] as follow:

$$K_{IC} \ (MPa \ \sqrt{m}) = \ 3(P_{Nmax} \ + \ 0.5mg)\frac{S\sqrt{\pi a}}{2d^2 \ b}f(\alpha) \tag{4}$$

Where P_{Nmax} is the maximum load on the notched prism in N, S is the span of the beam in m, α is the ratio of a and d, i.e., $\alpha = a/d = 0.35$ and $f(\alpha)$ is the geometry correction for bending load. A much accurate estimate of this parameter for varying specimen size, notch depth, and material property can be done using Finite Element Analysis[13]. But for simplicity and comparative analysis equation (5) is widely accepted and is used in the present study:

$$f(\alpha) = \frac{1.99 - \alpha(1-\alpha)(2.15 - 3.9\alpha + 2.7\alpha^2)}{\sqrt{\pi}(1+2\alpha)(1-\alpha)^{3/2}} \tag{5}$$
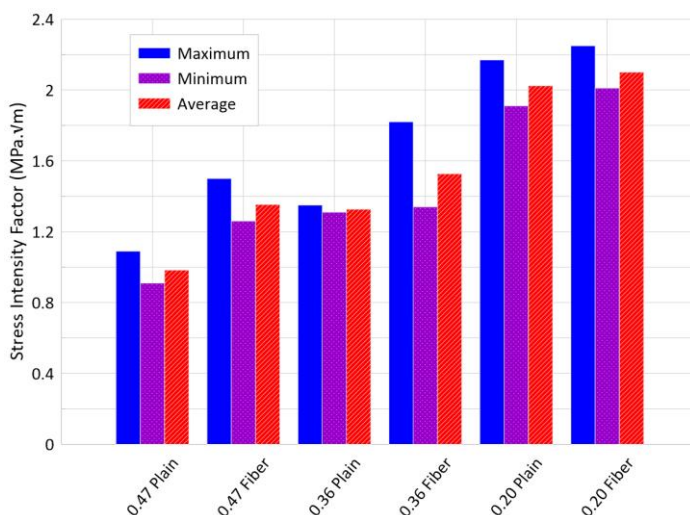

Fig. 14 Calculated stress intensity factor in the study

Figure 14 shows the values of the calculated stress intensity factor in the study. From the study, two important observations can be made. Firstly, adding steel fibers increases the stress intensity factor only marginally, this can be explained as fibers play a significant role only after a certain amount of crack has been made. Therefore, although fibers can significantly help arrest the cracks at a later stage, fiber only helps marginally in preventing initial cracks. Initial cracks formation in the beam depends on the tensile strength of the concrete which is related to the compressive strength and therefore a consistent increase in the stress intensity factor with compressive strength can be observed in the obtained result.

For a particular concrete sample, reported values of stress intensity factor in the literature [26] is about 1.14 MPa$\sqrt{m}$ for normal concrete which increases to 1.48 MPa$\sqrt{m}$ after the addition of steel fiber. Values, as well as the trend observed in our study, agrees with the literature.

5.6 Critical Energy Release Rate

The critical energy release rate, G_{IC}, is the rate at which energy is changed as the material gets fractured and creates a new surface. It can be mathematically defined as the decrease in total potential energy per increase in fracture surface area. For evaluating the material qualities related to fracture and fatigue, the energy release rate is a crucial factor. The equation given by Taha et al. [41] is used for calculating G_{IC} and is given in equation (6) as follow:

$$G_{IC}(N/m) = \frac{K_{IC}^2}{E} \tag{6}$$

The values of the calculated energy release rate are shown in figure 15. From the figure, a general trend can be observed that with the increase in concrete compressive strength a significant increase in energy release rate is observed. Therefore, with each new crack, a higher amount of strain energy is released for higher-strength concrete. The addition of fiber also increases the energy release rate but with the increase in concrete compressive strength, the percentage increase decreases. Similar to the stress intensity factor, this can be explained as at higher strength, the binder-aggregate mix is capable of taking a much higher load therefore the effect of fiber is slightly reduced compared to lower strength concrete.

The typical Energy release rate suggested in the literature [26] for normal concrete is 22.4 J/m^2, and for concrete with fiber is 100.2 J/m^2. Similar findings were observed for one of the samples in our analysis with a w/b ratio of 0.36.
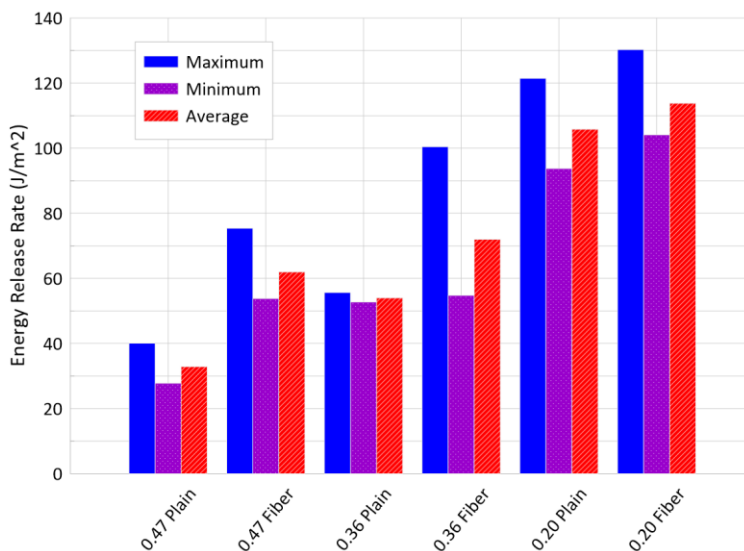

Fig. 15 Calculated energy release rate in the study

5.7 Characteristic Length

Characteristic length is a material parameter that reflects the lowest feasible breadth of a zone of strain-softening damage in nonlocal continuum formulations [42]. It can be understood as the minimum possible spacing of fractures in discrete fracture models. The principal idea behind finding the characteristic length is to compare the brittleness of two materials after the onset of initial cracks. Material with a smaller characteristic length can be considered more brittle, and crack can propagate easily in these materials. It can be calculated using the equation (7) provided by [43] as follows where E is young's modulus, G_f is fracture energy, and f_{st} is split tensile strength.

$$L_{ch}(mm) = \frac{EG_f}{f_{st}^2} \qquad (7)$$
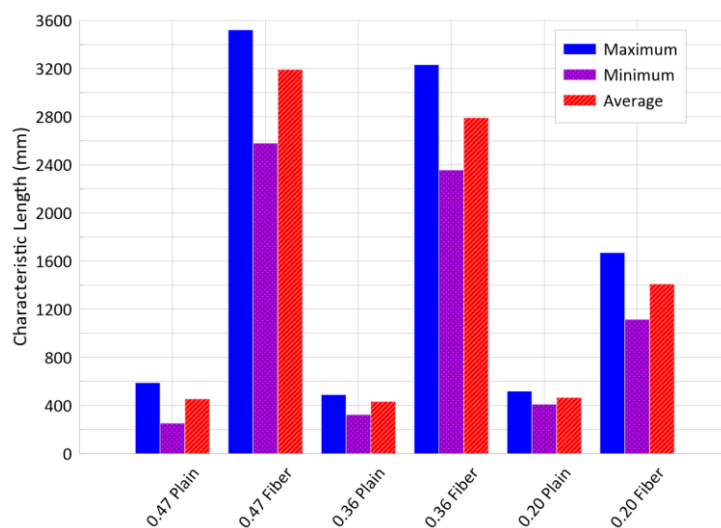
Fig. 16 Calculated Characteristic length of the study

The obtained values of the characteristic length in the study are presented in figure 16. From the figure, it can be observed that with an increase in compressive strength of concrete characteristic length decreases. Findings suggest that, for higher strength of concrete, Initial crack formation may be difficult due to higher stress intensity factor but crack propagation takes place much easily because cracks are less localized. Also, there is a large jump in the values of characteristic length after fiber addition. Therefore, it can be concluded that with the addition of fiber, concrete can have a much larger zone of strain-softening damage. This suggests that although crack may be initiated, but can be localized with the help of fiber addition. Past literature [26] also shows a massive jump in characteristic length from 806mm to 5382 mm when fiber was added to the concrete. A similar increase in the values in the characteristic strength was observed in our study.

6. Conclusions

In the present study, fracture parameters are evaluated for concrete mixes with w/b ratios of 0.47, 0.36, and 0.20 having a respective average compressive strength of 36 MPa,52 MPa, and 92 MPa without and with 1% steel fiber by volume. The three-point bending test method with central point loading is used in the study. Based on the analysis of the results following can be concluded from the study.

- Adding steel fibers significantly increase the fracture energy. The observed increase in fracture energy was 850%, 770%, and 450% respectively for a w/b ratio of 0.47, 0.36, and 0.20. Comparing concrete with different w/b ratios, with the increase in strength of concrete a consistent increase in the fracture energy is observed. The addition of fiber increases the strain carrying capacity of concrete and with the increase in concrete compressive strength, peak load in the load-deformation curve increases.
- Deterministic evaluation of the absolute value of the modulus of elasticity from the three-point bend test proposed by RILEM is extremely difficult due to the required level of sensitivity of the measurement. The Load-CMOD curve and initial compliance value are extremely sensitive and it requires accurate measurement of the order of 10^{-9} m in a mechanical bend test. Even a slight variation in the initial slope of the Load-CMOD curves leaves a magnified effect in the values of modulus of elasticity. Also, calculated values of modulus of elasticity were higher than established previous results. These values tend to become enormously high for higher strength concrete (for average compressive strength of 92 MPa). It can be suggested to limit this method only for comparative analysis and for absolute determination of modules of elasticity various other well-established procedures should be used.
- Stress intensity factor and energy release rate shows a similar trend and these two parameters improve with the addition of steel fiber but the observed increase is less when compared to increase in fracture energy. Results suggest that the compressive strength of concrete is an equally important factor for the increase in the values of these parameters along with the addition of fiber.
- Characteristic length of concrete shows an opposite trend from other parameters when concrete with different strengths is compared. For higher-strength concrete characteristic length is less. Comparing normal concrete with fiber reinforced concrete for a particular w/b ratio, a significant increase in characteristic length of the order of increase in fracture energy was observed.
- From the study it can be concluded that adding steel fiber tremendously increases the amount of energy needed for fracture of the beam. It also helps in arresting the cracks by increasing the characteristic length. But the formation of the initial crack is much closely related to the grade of concrete as fiber action can only be observed after the onset of initial cracks.

References

[1] Ojha P, Singh B, Singh A, Patel V, Arora VV. Experimental study on creep and shrinkage behaviour of high strength concrete for application in high rise buildings. Indian Concrete Journal, 2021; 95:2 30-42.
[2] Singh B, Arora VV, Patel V. Study on stress strain characteristics of high strength concrete. Indian Concrete Journal 2018; 92:6 37-43.
[3] Arora V.V., Singh Brijesh, Patel Vikas, Trivedi Amit. Evaluation of modulus of elasticity for normal and high strength concrete with granite and calc-granulite aggregate. Structural Concrete, 2021; 22:S1. https://doi.org/10.1002/suco.202000023
[4] Arora VV, Singh B, Jain S. Effect of indigenous aggregate type on mechanical properties of high strength concrete. Indian Concrete Journal 2017; 91:1 34-44.
[5] Arora VV, Singh B, Jain S. Experimental studies on short term mechanical properties of high strength concrete. Indian Concrete Journal 2016; 90:10 65-75.
[6] RILEM TC-50 FMC (Draft Recommendation). Determination of the fracture energy of mortar and concrete by means of three-point bend tests on notched beams. Mater Struct., 1985; 18:106 285-290. https://doi.org/10.1007/BF02472918

[7] Shah SP. Determination of fracture parameters (K Ic s and CTODc) of plain concrete using three-point bend tests. Materials and Structures, 1990; 23:6 457-460. https://doi.org/10.1007/BF02472029

[8] Patel V., Singh B., Arora V.V. Study on fracture behaviour of high strength concrete including effect of steel fiber. Indian Concrete Journal, 2020; 94:4 1-9.

[9] Trivedi N, Singh RK, Chattopadhyay J. A comparative study on three approaches to investigate the size independent fracture energy of concrete. Engineering Fracture Mechanics., 2015; 138: 49-62. https://doi.org/10.1016/j.engfracmech.2015.03.021

[10] Khalilpour S, BaniAsad E, Dehestani M. A review on concrete fracture energy and effective parameters, 2019. https://doi.org/10.1016/j.cemconres.2019.03.013

[11] Yin Y, Qiao Y, Hu S. Four-point bending tests for the fracture properties of concrete. Engineering Fracture Mechanics, 2019; 211: 371-381. https://doi.org/10.1016/j.engfracmech.2019.03.004

[12] Murthy AR, Ganesh P, Kumar SS, Iyerc NR. Fracture energy and tension softening relation for nano-modified concrete. Structural Engineering and Mechanics, 2015; 54:6 1201-1216. https://doi.org/10.12989/sem.2015.54.6.1201

[13] Kaya Z, Balcıoğlu HE, Gün H. The effects of temperature and deformation rate on fracture behavior of S-2 glass/epoxy laminated composites. Polymer Composites, 2020; 41:11 4799-4810. https://doi.org/10.1002/pc.25753

[14] Almusallam T, Ibrahim SM, Al-Salloum Y, Abadel A, Abbas H. Analytical and experimental investigations on the fracture behavior of hybrid fiber reinforced concrete. Cement and Concrete Composites, 2016; 74: 201-217. https://doi.org/10.1016/j.cemconcomp.2016.10.002

[15] Mousavi SM, Ranjbar MM, Madandoust R. Combined effects of steel fibers and water to cementitious materials ratio on the fracture behavior and brittleness of high strength concrete. Engineering Fracture Mechanics, 2019; 216. https://doi.org/10.1016/j.engfracmech.2019.106517

[16] Arslan ME. Effects of basalt and glass chopped fibers addition on fracture energy and mechanical properties of ordinary concrete: CMOD measurement. Construction and Building Materials, 2016; 114: 383-391. https://doi.org/10.1016/j.conbuildmat.2016.03.176

[17] Noaman AT, Abu Bakar BH, Akil HM, Alani AH. Fracture characteristics of plain and steel fibre reinforced rubberized concrete. Construction and Building Materials, 2017; 152: 414-423. https://doi.org/10.1016/j.conbuildmat.2017.06.127

[18] Wtaife S, Alsabbagh A, Shaban AM, Suksawang N. Fracture Mechanism of Fibre Reinforced Concrete Pavement Based on a RILEM Design Approach. In IOP Conference Series: Materials Science and Engineering. Institute of Physics Publishing (2020). https://doi.org/10.1088/1757-899X/671/1/012087

[19] Gil DM, Golewski GL. Effect of Silica Fume and Siliceous Fly Ash Addition on the Fracture Toughness of Plain Concrete in Mode i. In IOP Conference Series: Materials Science and Engineering. Institute of Physics Publishing (2018). https://doi.org/10.1088/1757-899X/416/1/012065

[20] Siregar APN, Rafiq MI, Mulheron M. Experimental investigation of the effects of aggregate size distribution on the fracture behaviour of high strength concrete. Construction and Building Materials, 2017; 150: 252-259. https://doi.org/10.1016/j.conbuildmat.2017.05.142

[21] Tang Y, Feng W, Chen Z, Nong Y, Guan S, Sun J. Fracture behavior of a sustainable material: Recycled concrete with waste crumb rubber subjected to elevated temperatures. Journal of Cleaner Production, 318 (2021). https://doi.org/10.1016/j.jclepro.2021.128553

[22] Yu K, Yu J, Lu Z, Chen Q. Fracture properties of high-strength/high-performance concrete (HSC/HPC) exposed to high temperature. Materials and Structures/Materiaux

et Constructions, 2016; 49:11 4517-4532. https://doi.org/10.1617/s11527-016-0804-x

[23] Tran NT, Tran TK, Jeon JK, Park JK, Kim DJ. Fracture energy of ultra-high-performance fiber-reinforced concrete at high strain rates. Cement and Concrete Research, 2016; 79: 169-184. https://doi.org/10.1016/j.cemconres.2015.09.011

[24] Guo M, Alam SY, Bendimerad AZ, Grondin F, Rozière E, Loukili A. Fracture process zone characteristics and identification of the micro-fracture phases in recycled concrete. Engineering Fracture Mechanics, 2017; 181: 101-115. https://doi.org/10.1016/j.engfracmech.2017.07.004

[25] Arora VV, Singh B. Use of Fly Ash Concrete and Recycled Concrete Aggregates-A Cost Effective Solution and Durable Option for Construction of Concrete Roads. Indian Concrete Journal, 2017; 91:1

[26] Alwesabi EAH, Bakar BHA, Alshaikh IMH, Zeyad AM, Altheeb A, Alghamdi H. Experimental investigation on fracture characteristics of plain and rubberized concrete containing hybrid steel-polypropylene fiber. Structures, 33 (2021). https://doi.org/10.1016/j.istruc.2021.07.011

[27] Al-Tayeb MM, Abu Bakar BH, Akil HM, Ismail H. Effect of Partial Replacements of Sand and Cement by Waste Rubber on the Fracture Characteristics of Concrete. Polymer - Plastics Technology and Engineering, 2012; 51:6. https://doi.org/10.1080/03602559.2012.659307

[28] Srawley JE. Wide range stress intensity factor expressions for ASTM E 399 standard fracture toughness specimens. International Journal of Fracture, 1976; 12:3. https://doi.org/10.1007/BF00032844

[29] Noaman AT, Abu Bakar BH, Akil HM, Alani AH. Fracture characteristics of plain and steel fibre reinforced rubberized concrete. Construction and Building Materials, 2017; 152: 414-423. https://doi.org/10.1016/j.conbuildmat.2017.06.127

[30] IS 516:2014. Method of Tests for Strength of Concrete. IS : 516 - 1959 (Reaffirmed 2004). (2004).

[31] Bureau of Indian Standards. Method of Test Splitting Tensile Strength of Concrete. IS 5816: 1999. (2018).

[32] Bureau of Indian Standards. Ordinary Portland Cement - Specification (Sixth Revision). (2015).

[33] Bureau of Indian Standards. Coarse and Fine Aggregate for Concrete - Specification (Third Revision). (2016).

[34] ASTM. Standard Specification for Steel Fibers for Fiber-Reinforced Concrete. A820/A820M.

[35] Bureau of Indian Standards. Specification for Concrete Admixtures. IS 9103-1999. (2018).

[36] Bureau of Indian Standards. Fresh Concrete: Methods of Sampling, Testing and Analysis Part 2 Determination of Consistency of Fresh Concrete (First Revision). IS 1199 (Part 2): 2018. (2018).

[37] Ojha PN, Trivedi A, Singh B, N S AK, Patel V, Gupta RK. High performance fiber reinforced concrete - for repair in spillways of concrete dams. Research on Engineering Structures and Materials, 2021. https://doi.org/10.17515/resm2021.252ma0128

[38] Singh B., Arora VV, Patel V. Experimental study on stress strain behaviour of normal and high strength unconfined concrete. Indian Concrete Journal, 2020; 94:4 10-19.

[39] Smarzewski P. Influence of silica fume on mechanical and fracture properties of high performance concrete. Procedia Structural Integrity, 2019; 17: 5-12. https://doi.org/10.1016/j.prostr.2019.08.002

[40] Javier Malvar L, Warren GE. Fracture energy for three point bend tests on single edge notched beams: Proposed evaluation. Materials and Structures, 1987; 20:6. https://doi.org/10.1007/BF02472495

[41] Reda Taha MM, El-Dieb AS, Abd El-Wahab MA, Abdel-Hameed ME. Mechanical, Fracture, and Microstructural Investigations of Rubber Concrete. Journal of Materials in Civil Engineering, 2008; 20:10. https://doi.org/10.1061/(ASCE)0899-1561(2008)20:10(640)

[42] Bažant ZP, Pijaudier-Cabot G. Measurement of Characteristic Length of Nonlocal Continuum. Journal of Engineering Mechanics, 1989; 115:4. https://doi.org/10.1061/(ASCE)0733-9399(1989)115:4(755)

[43] Şahin Y, Köksal F. The influences of matrix and steel fibre tensile strengths on the fracture energy of high-strength concrete. Construction and Building Materials, 2011; 25:4. https://doi.org/10.1016/j.conbuildmat.2010.11.084